Hysteresis of Colloid Retention and Release in Saturated Porous Media During Transients in Solution Chemistry

SAEED TORKZABAN,[‡]
HYUNJUNG N. KIM,[§] JIRI SIMUNEK,[‖]
AND SCOTT A. BRADFORD*,[†]

Earth Sciences Division, Lawrence, Berkeley National Laboratory, Berkeley, CA, Department Chemical and Environmental Engineering, University of California, Riverside, CA, Department Environmental Sciences, University of California, Riverside, CA, and USDA, ARS, U.S. Salinity Laboratory, Riverside, CA

Saturated packed column and micromodel transport studies were conducted to gain insight on mechanisms of colloid retention and release under unfavorable attachment conditions. The initial deposition of colloids in porous media was found to be a strongly coupled process that depended on solution chemistry and pore space geometry. During steady state chemical conditions, colloid deposition was not a readily reversible process, and micromodel photos indicated that colloids were immobilized in the presence of fluid drag. Upon stepwise reduction in eluting solution ionic strength (IS), a sharp release of colloids occurred in each step which indicates that colloid retention depends on a balance of applied (hydrodynamic) and resisting (adhesive) torques which varied with pore space geometry, surface roughness, and interaction energy. When the eluting fluid IS was reduced to deionized water, the final retention locations occurred near grain–grain contacts, and colloid aggregation was sometimes observed in micromodel experiments. Significant amounts of colloid retention hysteresis with IS were observed in the column experiments, and it depended on the porous medium (glass beads compared with sand), the colloid size (1.1 and 0.5 μm), and on the initial deposition IS. These observations were attributed to weak adhesive interactions that depended on the double layer thickness (e.g., the depth of the secondary minimum and/or nanoscale heterogeneity), colloid mass transfer on the solid phase to regions where the torque and force balances were favorable for retention, the number and extent of grain–grain contacts, and surface roughness.

Introduction

Many environmentally relevant particles such as microorganisms, clays, and collectors (i.e., porous media) are negatively charged at the prevailing pH conditions (*1*). In this case, Derjaguin–Landau–Verwey–Overbeek (DLVO) theory (*2, 3*) indicates the presence of a significant energy barrier against colloid attachment in the primary minimum due to electrostatic repulsion. Nevertheless, a finite amount of colloids are still retained in porous media under these unfavorable attachment conditions. Potential adhesive interactions include the secondary minimum (e.g., refs *4, 5*) and nanoscale heterogeneity (*6–8*). Secondary minimum interaction may occur at a separation distance of a few nm from the collector surface due to the summation of electrostatic repulsion and van der Waals attraction. Chemical or physical nanoscale heterogeneities that are much smaller than the diameter of the colloid–surface contact area may also create favorable patches for interaction. This interaction occurs at a separation distance from the collector surface due to electrostatic repulsion from neighboring regions. It should be mentioned that colloid interaction via the secondary minimum and nanoscale heterogeneity share many similarities in that they function at a separation distance, the interaction strength will be a function of the double layer thickness (ionic strength), and the interaction is relatively weak in comparison to the primary minimum.

It has recently been demonstrated that colloid retention does not solely depend on the strength of the adhesive interaction as previously postulated (*9–13*). These new findings suggest that pore structure and hydrodynamic forces along with the physicochemical factors strongly affect colloidal retention. In particular, it has been reported that weakly associated colloids with the solid–water interface via the secondary minimum or nanoscale heterogeneity may experience significant hydrodynamic forces due to fluid flow that may result in rolling, sliding, skipping, or detachment of colloids on/from the collector surface (*9–11, 14, 15*). Some of these weakly associated colloids can be translated and/or funneled by fluid drag force to low velocity regions in small pore spaces and "eddy zones" which occur near some grain–grain contacts and surface roughness locations where they can be retained (*10, 12*). Indeed, recent experimental evidence by Kuznar and Elimelech (*14*) demonstrates that weakly interacting colloids can be translated along the collector surface via hydrodynamic forces and be retained in regions near the rear stagnation point.

Although colloid interaction with porous media via the secondary minimum and nanoscale heterogeneity are gaining wide acceptance (*6–13, 15–18*), our understanding of these weak interactions is still incomplete. For example, some recent literature indicates that colloids associated with solid surfaces via the secondary minimum are "freely mobile" in the presence of fluid drag (*19, 20*), whereas others have indicated that immobilization and detachment of these colloids will depend on a balance of applied (hydrodynamic) and resisting (adhesive) torques and forces (*9–13*). These subtle differences in the conceptual description of colloid interaction have important implications for colloid deposition and release that will be discussed in detail later on. Furthermore, hysteresis in the amount of colloid retention with IS has been observed over limited experimental conditions (*21–23*). The nature and cause for this hysteresis is still not well understood. To the best of our knowledge, to date, no published studies have systematically investigated colloid retention hysteresis over a range of IS. One logical way to investigate these issues is to study the influence of transients in solution IS on colloid release. Switching the eluting fluid to a lower IS has been observed to enhance colloid release due to increased electrostatic repulsion and a corresponding

* Corresponding author phone: 951-369-4857; e-mail: Scott.Bradford@ars.usda.gov.
  [†] U.S. Salinity Laboratory.
  [‡] Lawrence, Berkeley National Laboratory.
  [§] Department Chemical and Environmental Engineering, University of California.
  [‖] Department Environmental Sciences, University of California.

TABLE 1. Porous Media Experimental Conditions and Mass Balances[a]

d_c (μm)	porous media	IS (mM)	approach velocity (cm/min)	column length (cm)	PV_0	BTC %	mass recovery %
1.1	glass beads	6	0.2	5	5.2	99	100
		16	0.2	5	5.2	98	99
		36	0.2	5	5.2	85	93
		66	0.2	5	5.2	70	86
		106	0.2	5	5.2	37	83
	Ottawa sand	6	0.2	5	6.1	98	100
		16	0.2	5	3.5	73	97
		66	0.2	5	6.5	10	64
0.5	glass beads	16	0.1	10	5.4	84	99
		66	0.1	10	5.3	20	50
	Ottawa sand	16	0.1	10	3.5	61	97
		66	0.1	10	5.2	4	41

[a] d_c, colloid diameter; IS, ionic strength; PV_0, colloid pulse during phase A in terms of pore volumes; BTC (%), percent recovery of injected colloids during the phases A and B; Mass recovery (%), percent recovery of injected colloids during phases A, B, and C.

increase in the double layer thickness (*21–24*). However, wide discrepancies in the extent, rate, and shape of release have been reported (*10, 21–23*).

The literature review above indicates that our understanding of the coupled role of solution chemistry, fluid hydrodynamics, pore structure, and surface heterogeneity on colloid retention and release is still incomplete under unfavorable conditions. The overall research objective of this work is to provide experimental evidence and improved understanding of colloid retention and release under unfavorable attachment conditions. Findings from this work provided valuable information on plausible mechanisms of colloid retention, the resisting (adhesive) torque, colloid retention hysteresis with IS, and colloid mass transfer on the solid phase. All of this information increases our knowledge of factors that influence colloid release with transients in solution chemistry in natural environments.

Material and Methods

Colloid, Electrolyte Solution, and Porous Media. Carboxylate-modified polystyrene latex microspheres (Molecular Probes, Inc., Eugene, Oregon) of two sizes (diameters of 0.5 and 1.1 μm with negative surface charge densities of 0.1419 and 0.0175 meq g^{-1}, respectively) were used in the experiments. Aqueous solutions used in the experiments consisted of deionized (DI) water with its pH adjusted to 10 using 1.7 mM of Na_2CO_3 and 1.7 mM of $NaHCO_3$. The IS was adjusted to desired levels using NaCl. The concentration of colloid suspension ($2.5-2.8 \times 10^7$ N_c ml^{-1}; where N_c denotes number of colloids) was selected to minimize any permeability reductions of the porous medium. Ottawa sand (U.S. Silica, Ottawa, IL) and spherical soda lime glass beads (USF Surface Preparation, Rancho Dominguez, CA) were used as porous media. Ottawa sand and glass beads have median grain sizes (d_{50}) of 240 and 260 μm, respectively. The uniformity indexes ($U_i = d_{60}/d_{10}$ where x% of the mass was finer than d_x) of the sand and glass beads were measured to be 3.06 and 1.20, respectively. Ottawa sand typically consists of 99.8% SiO_2 (quartz) and trace amounts of metal oxides. Table 1 indicates the parameters of each column experiment.

DLVO Calculations. Colloid–colloid and colloid–collector interaction energy profiles were calculated using DLVO theory (*2, 3*) as described in the Supporting Information (SI) for the two microsphere sizes (0.5 and 1.1 μm) in the various solution chemistries.

Transport Experiment Protocol. A stainless steel column with internal diameter of 5 cm was selected for this study. The packing and pre-equilibration procedures for each column experiment is described in a previous publication

(*25*). The porosity of the packed columns was determined gravimetrically and it varied between 35 and 38%. After establishing specified water chemistry, transport experiments were carried out in three phases. In phase A colloid suspension was introduced into the column at a constant rate. The colloid suspension was applied for a given number of pore volumes (PV_0) provided in Table 1. During injection, the colloid suspension reservoir was agitated to minimize aggregation, as verified by absorbance analyses. During phase B colloid-free electrolyte solution was applied to the column at the same flow rate and IS as during phase A until the effluent colloid concentration returned to a baseline level. Finally, the influent IS was lowered in several steps (to study mobilization/release behavior of colloids) during phase C. After changing the IS in each step, the column was flushed with the lowered IS solution until the change in effluent concentration was minimal. During the transport experiment, effluent samples were collected at selected intervals by a fraction collector and analyzed for colloid concentration using a spectrophotometer (Perkin-Elmer LC95 UV/vis spectrophotometer, Irvine, CA) at a wavelength of 480 nm. The colloid mass recovery (%) was calculated as the ratio of the amount of eluted colloids during all three stages to the amount of introduced colloids

Micromodel Experiments. Transport experiments were also conducted in a specially designed micromodel (*26*) to microscopically examine the retention and release behavior of colloids in the porous media at different ISs. Details on experimental micromodel procedures are given in Bradford et al. (*26*) and the SI.

Results

DLVO Calculations. Table S1 in the SI presents calculated colloid–colloid and colloid–collector interaction energies from DLVO theory when the solution ISs were 15, 60, and 100 mM. Results indicate that colloid–colloid and colloid–collector interactions are repulsive for both colloids (0.5 and 1.1 μm). However, it can be observed that the depth of the secondary energy minimum and the height of the repulsive energy barriers increases and decreases, respectively, with increasing IS. Diffusion of colloids over these energy barriers is reported to be highly unlikely (*27*). Hence, DLVO calculations indicate unfavorable attachment conditions for the primary minimum, but a potential for a weak association via the secondary minimum.

Colloid Deposition and Release in Column Studies. Figure 1 presents representative colloid breakthrough concentrations (BTCs) in the effluent (during phases A and B) obtained from columns packed with glass beads at the various
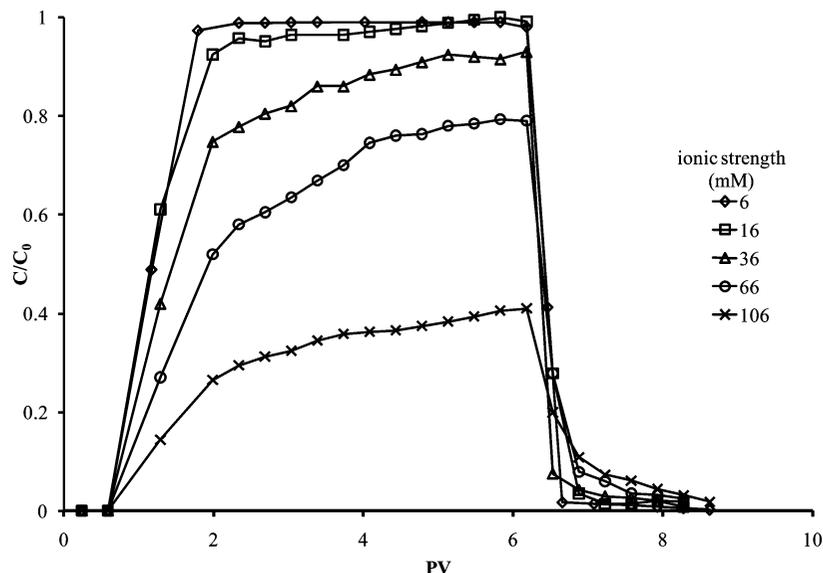
FIGURE 1. Breakthrough curves for 1.1 μm latex colloids in glass beads when the Darcy velocity was approximately 0.2 cm min^{-1}, the pH was 10, and the ionic strength was 6, 16, 36, 66, and 106 mM. Here the normalized effluent concentration (C/C_0) is plotted as a function of pore volumes (PV) passed through the column.

solution ISs. Here the normalized effluent concentration (C/C_0) is plotted as a function of pore volumes (PV) passed through the column. An increase in IS resulted in enhanced colloid deposition, consistent with previous column transport studies that involved a variety of colloidal particles and porous media (*4, 5, 10, 17*). The time dependent trend observed in the rising limb of the BTC indicates that either the retention sites were being filled up during colloid injection (blocking) or simultaneous release (detachment) of deposited colloids was occurring during the transport experiment. However, blocking or filling of available locations for deposition seems to be a more likely explanation because colloid detachment produced insignificant tailing in the BTCs.

The BTCs obtained from experiments conducted with Ottawa sand (SI Figure S1) exhibited a similar trend with IS as shown in Figure 1, however more colloid retention occurred in the sand columns compared with the glass beads at a given IS. Table 1 presents the recovery (%) of injected 0.5 and 1.1 μm colloids during phases A and B (referred to as BTC%) for both glass bead and Ottawa sand at the various ISs. Most of these colloid transport experiments were conducted in duplicate at each IS, and exhibited good reproducibility.

Figure 2 presents typical behavior of colloid release after lowering the influent IS in several steps during phase C. The results of other transient IS experiments are summarized in Table 2. A sudden peak in effluent concentration was observed following a decrease in solution IS. Further comparison of the release data with tracer experiments suggests that the step change in solution IS resulted in a rapid, pulse-like release of colloids that appears within the front of the solution with lower IS. However, the colloid concentration in the effluent sharply dropped after the front and exhibited a small tail. A significant amount of released particles occurred when the influent was switched to DI water at the last step. However, the mass recovery data (Table 2) shows that a significant fraction of the deposited colloids was not released in the experiments at higher ISs (i.e., 66 and 106 mM) even after flushing the column with DI water. To further investigate the possible recovery of the retained colloids, a flow interruption of 12 up to 24 h was applied for select experiments. To our surprise, the results showed that only a very small fraction of the remaining colloids was recovered after the flow was restarted.

Figure 3 summarizes the colloid retention data at the various ISs for the 1.1 μm colloids in glass beads and Ottawa sand. Here the percentages of retained colloids are plotted as a function of the solution IS history. The arrows indicate the direction of the IS change, with arrows facing to the right indicating results obtained during phases A and B, whereas those facing to the left for phase C. Figure 3 clearly indicates that the amount of colloid retention at a given IS was a function of the solution IS history. In particular, observe that the amount of colloid retention at a given IS increased as the initial IS increased during phases A and B. Furthermore, the Ottawa sand has much greater colloid retention than the glass beads for a similar IS history. These findings hold for both 1.1 and 0.5 μm colloids (Table 2), although exact comparison of these results is not possible due to differences in the column length and the approach velocity (Table 1). To the best of our knowledge, this is the first study to systematically demonstrate colloid retention hysteresis for various ISs, porous media types, and colloid sizes.

Colloid Deposition and Release in Micromodel Studies. Micromodel studies were conducted to better understand the factors influencing the observed colloid retention hysteresis. Figure 4 presents micromodel photos of retained colloids in glass beads when the initial deposition (phases A and B) was conducted at a solution IS of 106 mM, and then the eluting solution IS was decreased in a stepwise fashion to 66, 31, 6, and 0 (DI water) mM (phase C). The photos demonstrate that the retained colloids were relatively uniformly distributed on the collector surfaces when the ISs were 106, 66, 31, and 6 mM. In contrast, under DI water conditions colloid retention was only possible (almost exclusively) near grain−grain contact points. A similar micromodel experiment to that described above was conducted using Ottawa sand (SI Figure S2). The observations were comparable with those for the glass beads.

Discussion

Results presented in Figures 1−4 provide valuable information to better understand the nature of underlying mechanisms for colloid deposition and release under unfavorable attachment conditions. Discussion provided in the SI indicates that irreversible retention of colloids in the primary minimum is likely to play only a minor role in colloid retention under the selected experimental conditions. Below we will
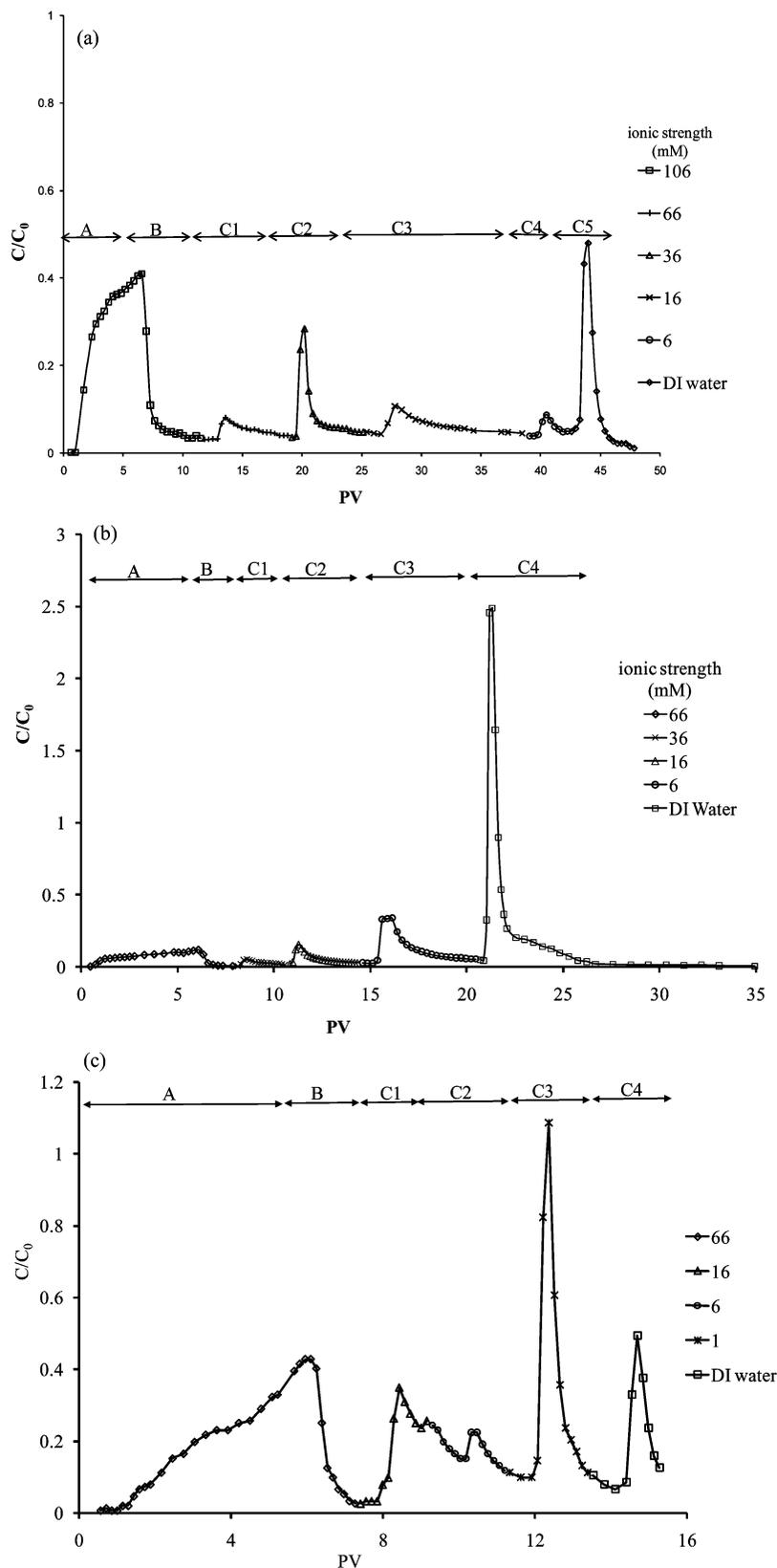
FIGURE 2. Representative plots of the relative effluent concentration (C/C_0) as a function of pore volumes (PV) for transient ionic strength (IS) experiments. Figure 2a and b were for 1.1 μm latex microspheres in glass beads and Ottawa sand, respectively, and Figure 2c for 0.5 μm colloids in glass beads. The sequence of the transient experiments was (i) deposition of colloids in the column during phase A; (ii) elution with the same electrolyte solution (without colloids) during phase B; and (iii) the eluting solution IS was lowered in several steps indicated in the figure legend during phase C. Other experimental conditions are summarized in Tables 1 and 2.

examine two potential explanations for observed colloid retention and release during transient in IS, namely: interac-

tion in the secondary minimum, and nanoscale surface roughness and chemical heterogeneity.

d_c (μm)	porous media	initial IS (mM)	cumulative mass recovery in effluent (%)					
			106 mM	66 mM	36 mM	16 mM	6 mM	DI
1.1	glass beads	6					99	100
		16				98	99	99
		36			85	86	90	94
		66		70	71	73	78	86
		106	37	43	52	66	72	83
	Ottawa sand	6					98	100
		16				73		97
		66		10	11	15	28	64
0.5	glass beads	16				84	90	100
		66		20	20	26	32	49
	Ottawa sand	16				61	71	96
		66		4	8	13	28	41

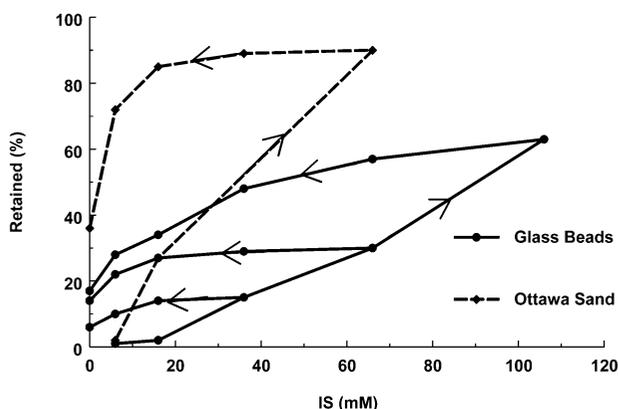[a] d_c, colloid diameter; IS, ionic strength; DI, deionized water.

FIGURE 3. A summary of the colloid retention data during the transient IS experiments for the 1.1 μm colloids in glass beads and Ottawa sand. Here the percentages of retained colloids are plotted as a function of the solution IS history. The arrows indicate the direction of the IS change, with arrows facing to the right indicating results obtained during phases A and B, whereas those facing to the left for phase C.

Secondary Minimum. Table S1 in the SI indicates the presence of a secondary minimum for all of the conditions considered herein. Figure 2 indicates that colloid release occurred in a stepwise fashion with IS. This observation is consistent with the assumption of a resisting (adhesive) torque and force for colloids associated with the solid surface via the secondary minimum (9–11, 13). Furthermore, the experimental observations show a sharp peak of colloid release upon virtually complete removal of the secondary minimum (DI water). Hence, the deposited colloids were not exclusively retained in zones of "flow stagnation" as has sometimes been assumed in the literature (19, 20) because the colloid release was not diffusion controlled.

The fraction of the collector surface that is "chemically and hydrodynamically" favorable for colloid retention (S_f) may be determined using the torque balance approach assuming rolling is the dominant detachment mechanism (9, 10). In the absence of surface roughness and chemical heterogeneity, this approach predicts that S_f decreases with decreasing IS in a nonlinear fashion, and that retention occurs in progressively lower velocity regions of the pore space. Torque balance calculations indicate that low velocity regions near some grain−grain contacts are usually hydrodynamically favorable for retention (10). This prediction is supported by micromodel observations shown in Figure 4 under DI water conditions when the secondary minimum was eliminated. In contrast, Figure 4 indicates that the retained colloids were relatively uniformly distributed on the collector surfaces when the IS was decreased in a stepwise fashion from 106, 66, 31, to 6 mM.

Surface roughness has also been demonstrated to play an important factor in colloid retention (28, 29). Surface roughness locations may influence the applied hydrodynamic force and torque. In particular, when the roughness is greater than the colloid radius, the applied hydrodynamic torque will be zero (30), and create locations that are hydrodynamically favorable for retention (similar to regions near grain−grain contacts) even under very low values of IS. Smart and Leighton (31) reported that the surface roughness of glass beads is approximately 0.01 to 0.001 times the bead radius depending on the manufacturing process. This yields an estimate of surface roughness ranging from 1.3 to 0.13 μm. Hence, surface roughness provides one plausible explanation for the relatively uniform distribution of retained colloids shown in Figure 4 when IS > 0 mM. Differences in the diffusion distance at grain−grain contacts and surface roughness may help to explain the relatively large pulse of colloid release when the IS was changed from 6 mM to DI water in Figure 2 as the depth of secondary minimum was completely eliminated.

The observed hysteresis in colloid retention can be explained in part by colloid mass transfer on the solid phase as will be discussed below. Filtration theory (32) predicts that the amount of colloid retention during phase A will depend primarily on the collector efficiency (η) and the sticking efficiency (α). The value of η is related to the mass transfer rate of colloids toward the solid phase and is typically quantified using correlation equations (e.g., ref 33). The value of α is the probability that colloids colliding with the collector will remain associated with the solid (24). Under unfavorable attachment conditions the value of α has been estimated from the depth of the secondary minimum and the distribution of kinetic energies associated with diffusing colloids (34). In this case, the value of α is predicted to increase in a nonlinear fashion with IS. This approach, however, neglects the influence of hydrodynamics and pore structure on colloid retention. Colloids that collide with the solid surface and become weakly associated with the surface via the secondary minimum can be translated and/or funneled by fluid drag forces to low velocity regions and "eddy zones" near grain−grain contact points and surface roughness locations. A larger number of colloids may entered these low velocity regions at higher IS due to the greater depth of secondary minimum.

The amount of colloid mass transfer on the solid surface during phases A and B is therefore expected to be greater
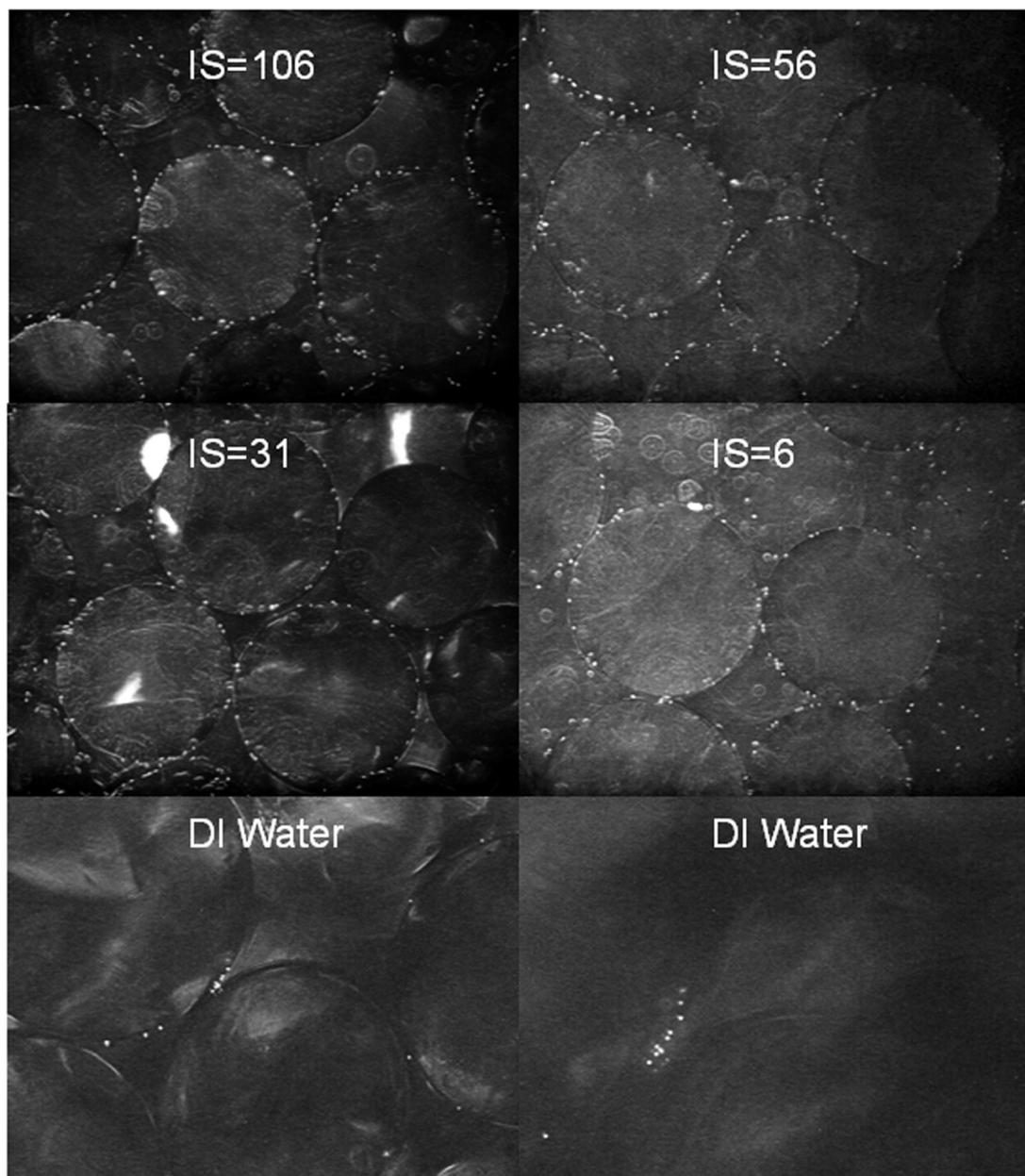
FIGURE 4. Representative photos of 1.1 µm colloid retention in the glass beads during the various ionic strength (IS) stages of a transient micromodel experiment. The initial deposition stage occurred at an IS of 106 mM, and then the eluting solution IS was lowered in a stepwise fashion to 56, 31, 6, and 0 mM solutions. The Darcy velocity was 0.2 cm min^{-1}, and the flow was from the left to the right.

with increasing IS. It is likely that some of the colloids being transported on the solid surface and even a fraction of the detached colloids during phase C may be subsequently deposited in the low velocity regions. This hypothesis is supported by results shown in Figure 3 in that the difference in the amount of colloid retention at a given IS increased with the deviation in the initial (phases A and B) and final (phase C) IS conditions. This trend is more pronounced at high ISs due to the nonlinear dependence of colloid mass transfer on the solid surface with IS (9, 10, 30). The observed differences in the colloid retention hysteresis for glass beads and Ottawa sand (Figure 4) may be due to the fact that the irregular shape and surface roughness of the Ottawa sand has a greater length and number of low velocity regions compared with that of spherical glass beads that produces a larger value of S_f (35).

Table 1 presents the mass recovery of introduced colloids in the effluent after the completion of the transient IS experiments. Even after elimination of the secondary mini-

mum following a rinse with DI water and flow interruption, only a fraction of the input colloids was recovered in the effluent for the experiments conducted at high ISs such as 66 and 106 mM. One potential explanation is due to the aggregation of those colloids trapped in low velocity regions. Micromodel observations sometimes indicated that colloid aggregation may have occurred near grain–grain contacts (see for example the bottom right-hand photo in Figure 4). Similarly, Bradford et al. (36) and Tong et al. (37) visually observed that colloid aggregation occurred near grain-to-grain contact points under unfavorable conditions. It is plausible that colloid aggregation is facilitated by confinement in hydrodynamically isolated regions near grain-to-grain contact points due to an increased probability of collision and hydrodynamic forces. In other words, the funneling of colloids into these low velocity regions may allow free colloids to overcome repulsion between each other, and produce aggregation. Hence, aggregation is likely to be in part

responsible for the observed incomplete effluent mass recovery of colloids.

Nanoscale Surface Roughness and Chemical Heterogeneity. The observed colloid transport and retention behavior may be explained by the combination of secondary minimum interaction, mass transfer, pore structure, surface roughness, and aggregation as described above. An alternative hypothesis for colloid retention under unfavorable conditions is nanoscale chemical and/or physical (roughness) heterogeneity.

Nanoscale chemical heterogeneity (6–8, 15, 18, 38–40) is assumed to be much smaller in size than the colloidal particles. In this case, the interaction force from neighboring regions will have a significant effect on the adhesive force and resisting torque that act on colloids near solid surfaces (18). These nanoscale chemical heterogeneities have been demonstrated to produce attachment on surfaces, even when the average charge properties are unfavorable for attachment (39, 40). Results presented by Duffadar and Davis (18) indicate that the magnitude of the attractive electrostatic force between the colloid and the "favorable nanoscale patches" increases with IS due to compression of the double layer thickness and is also a function of the colloid size. Similar to the secondary minimum discussed above, colloids may interact with "favorable nanoscale patches" at a separation distance, and results in attachment, detachment or rolling on the solid surface depending on the local hydrodynamics, the density and charge of the nanoscale patches, and the Brownian force (38). Hence, it is logical to expect that colloid attachment to "favorable nanoscale patches" is a function of the IS. Specifically, a larger number of colloids may interact with "favorable nanoscale patches" at a thinner (higher IS) than a thicker (lower IS) double layer as they move near the solid surface and find a local minima in the interaction energy. Furthermore, in contrast to the secondary minimum attachment, it is logical to anticipate that it would be more difficult to detach colloids from local minima found under higher than lower IS conditions by changing the solution chemistry or hydrodynamic force. This phenomenon might also cause colloid retention hysteresis.

It should also be mentioned that repulsive interaction between a colloidal particle and a solid surface is lower on a rough surface compared to a smooth surface (41). The reduction in the energy barrier is strongly correlated with the magnitude of nanoscale surface roughness (41). Similar to nanoscale chemical heterogeneity, these findings suggest that surface roughness can create locally favorable conditions for colloid deposition on macroscopically unfavorable substrates. It is possible that nanoscale surface roughness and nanoscale chemical heterogeneity may influence colloid adhesive interactions in a similar way. Nanoscale chemical and physical heterogeneity also provides an alternative explanation to the relatively uniform distribution of retained colloids when the IS ≥ 6 mM (Figure 4), for the incomplete recovery of the colloids in DI water (i.e., complete elimination of secondary minimum) following periods of flow interruption, and for the observed colloid retention hysteresis. The relative importance of secondary minimum, nanoscale heterogeneity, and surface roughness on colloid retention is difficult to quantify, and the above discussion suggests all of these factors are likely to play a role and to function in a similar manner.

Supporting Information Available

A brief description and discussion of (i) the DLVO calculations and results; (ii) the micromodel procedures and results for Ottawa sand; (iii) representative colloid breakthrough curves for different IS in the Ottawa sand; and (iv) discussion related to the potential for colloids to interact via the primary minimum. This material is available free of charge via the Internet at http://pubs.acs.org.

Literature Cited

(1) Wan, J. M.; Tokunaga, T. K. Partitioning of clay colloids at air-water interfaces. *J. Colloid Interface Sci.* **2002**, *247*, 54–61.

(2) Derjaguin, B. V.; Landau, L. D. Theory of the stability of strongly charged lyophobic sols and of the adhesion of strongly charged particles in solutions of electrolytes. *Acta Physicochim. U.S.S.R.* **1941**, *14*, 733–762.

(3) Verwey, E. J. W.; Overbeek, J.Th.G. *Theory of the Stability of Lyophobic Colloids*; Elsevier: Amsterdam, 1948.

(4) Franchi, A.; O'Melia, C. R. Effects of natural organic matter and solution chemistry on the deposition and reentrainment of colloids in porous media. *Environ. Sci. Technol.* **2003**, *37* (6), 1122–1129.

(5) Hahn, M. W.; Abadzic, D.; O'Melia, C. R. Aquasols: On the role of secondary minima. *Environ. Sci. Technol.* **2004**, *38*, 5915–5924.

(6) Adamczyk, Z.; Michna, A.; Szaraniec, M.; Bratek, A.; Barbasz, J. Characterization of poly(ethylene imine) layers on mica by the streaming potential and particle deposition methods. *J. Colloid Interface Sci.* **2007**, *313*, 86–96.

(7) Adamczyk, Z.; Zembala, M.; Michna, A. Polyelectrolyte adsorption layers studied by streaming potential and particle deposition. *J. Colloid Interface Sci.* **2006**, *303*, 353–364.

(8) Kozlova, N.; Santore, M. M. Micron-scale adhesion dynamics mediated by nanometer-scale surface features. *Langmuir* **2006**, *22*, 1135–1142.

(9) Torkzaban, S.; Bradford, S. A.; Walker, S. L. Resolving the coupled effects of hydrodynamics and DLVO forces on colloid attachment to porous media. *Langmuir* **2007**, *23*, 9652–9660.

(10) Torkzaban, S.; Tazehkand, S. S.; Walker, S. L.; Bradford, S. A. Transport and fate of bacteria in porous media: Coupled effects of chemical conditions and pore space geometry. *Water Resour. Res.* **2008**, *44*, article no. W04403, DOI: 10.1029/2007WR006541.

(11) Bradford, S. A.; Torkzaban, S.; Walker, S. L. Coupling of physical and chemical mechanisms of colloid straining in saturated porous media. *Water Res.* **2007**, *41*, 3012–3024.

(12) Shen, C.; Huang, Y.; Li, B.; Jin, Y. Effects of solution chemistry on straining of colloids in porous media under unfavorable conditions. *Water Resour. Res.* **2008**, *44*, W05419, DOI: 10.1029/2007WR006580.

(13) Bradford, S. A.; Torkzaban, S. Colloid transport and retention in unsaturated porous media: A review of interface, collector, and pore scale processes and models. *Vadose Zone J.* **2008**, *7*, 667–681.

(14) Kuznar, Z. A.; Elimelech, M. Direct microscopic observation of particle deposition in porous media: Role of the secondary energy minimum. *Colloids Surf., A* **2007**, *294*, 156–162.

(15) Duffadar, R. D.; Davis, J. M. Interaction of micrometer-scale particles with nanotextured surfaces in shear flow. *J. Colloid Interface Sci.* **2007**, *308*, 20–29.

(16) Redman, J. A.; Walker, S. L.; Elimelech, M. Bacterial adhesion and transport in porous media: role of the secondary energy minimum. *Environ. Sci. Technol.* **2004**, *38*, 1777–1785.

(17) Tufenkji, N.; Elimelech, M. Breakdown of colloid filtration theory: role of the secondary energy minimum and surface charge heterogeneities. *Langmuir* **2005**, *21*, 841–852.

(18) Duffadar, R. D.; Davis, J. M. Dynamic adhesion behavior of micrometer-scale particles flowing over patchy surfaces with nanoscale electrostatic heterogeneity. *J. Colloid Interface Sci.* **2008**, *326*, 18–27.

(19) Johnson, W. P.; Li, X.; Yal, G. Colloid retention in porous media: Mechanistic confirmation of wedging and retention in zones of flow stagnation. *Environ. Sci. Technol.* **2007**, *41*, 1279–1287.

(20) Yang, C.; Dabros, T.; Li, D.; Czarnecki, J.; Masliyah, J. H. Kinetics of particle transport to a solid surface from an impinging jet under surface and external force fields. *J. Colloid Interface Sci.* **1998**, *208*, 226–240.

(21) Ryan, J. N.; Gschwend, P. M. Effect of ionic strength and flow rate on colloid release: Relating kinetics to intersurface potential energy. *J. Colloid Interface Sci.* **1994**, *164*, 21–34.

(22) Bergendahl, J.; Grasso, D. Prediction of colloid detachment in a model porous media: Thermodynamics. *AIChE J.* **1999**, *45*, 475–484.

(23) Lenhart, J. J.; Saiers, J. E. Colloid mobilization in water-saturated porous media under transient chemical conditions. *Environ. Sci. Technol.* **2003**, *37*, 2780–2787.

(24) Ryan, J. N.; Elimelech, M. Colloid mobilization and transport in groundwater. *Colloids Surf., A.* **1996**, *107*, 1–56.

(25) Torkzaban, S.; Bradford, S. A.; van Genuchten, M. Th.; Walker, S. L. Colloid transport in unsaturated porous media: The role of water content and ionic strength on particle straining. *J. Contam. Hydrol.* **2008**, *96*, 113–128.

(26) Bradford, S. A.; Simunek, J.; Bettahar, M.; Tadassa, Y. F.; van Genuchten, M. Th.; Yates, S. R. Straining of colloids at textural interfaces. *Water Resour. Res.* **2005**, *41*, W10404, DOI: 10.1029/2004WR003675.

(27) Shen, C.; Li, B.; Huang, Y.; Jin, Y. Kinetics of coupled primary- and secondary-minimum deposition of colloids under unfavorable chemical conditions. *Environ. Sci. Technol.* **2007**, *41*, 6976–6982.

(28) Yoon, J. S.; Germaine, J. T.; Culligan, P. J. Visualization of particle behavior with a porous medium: Mechanisms for particle filtration and retardation during downward transport. *Water Resour. Res.* **2006**, *42*, W06417, DOI: 10.1029/2004WR003660.

(29) Choi, N. C.; Kim, D. J.; Kim, S. B. Quantification of bacterial mass recovery as a function of pore-water velocity and ionic strength. *Res. Microbiol.* **2007**, *158*, 70−78.

(30) Vaidyanathan, R.; Tien, C. Hydrosol deposition in granular beds. *Chem. Eng. Sci.* **1988**, *43*, 289–302.

(31) Smart, J. R.; Leighton, D. T. Measurement of the hydrodynamic surface roughness of noncolloidal spheres. *Phys. Fluids A* **1989**, *1*, 52–60.

(32) Yao, K. M.; Habibian, M. T.; O'Melia, C. R. Water and waste water filtration: Concepts and applications. *Environ. Sci. Technol.* **1971**, *5*, 1105–1112.

(33) Tufenkji, N.; Elimelech, M. Correlation equation for predicting single-collector efficiency in physiochemical filtration in saturated porous media. *Environ. Sci. Technol.* **2004**, *38*, 529–536.

(34) Simoni, S. F.; Harms, H.; Bosma, T. N. P.; Zehnder, A. J. B. Population heterogeneity affects transport of bacteria through sand columns at low flow rates. *Environ. Sci. Technol.* **1998**, *32*, 2100–2105.

(35) Johnson, W. P. Excess colloid retention in porous media as a function of colloid size, fluid velocity, and grain angularity. *Environ. Sci. Technol.* **2006**, *40*, 7725–7731.

(36) Bradford, S. A.; Simunek, J.; Walker, S. L. Transport and deposition of E. coli O157:H7 in saturated porous media. *Water Resour. Res.* **2006**, *42*, W12S12, DOI: 10.1029/2005WR4805.

(37) Tong, M.; Ma, H.; Johnson, W. P. Funneling of flow into grain-to-grain contacts drives colloid-colloid aggregation in the presence of an energy barrier. *Environ. Sci. Technol.* **2008**, *42*, 2826–2832.

(38) Duffadar, R.; Kalasin, S.; Davis, J. M.; Santore, M. M. The impact of nanoscale chemical features on micron-scale adhesion: crossover from heterogeneity-dominated to mean field behavior. *J. Colloid Interface Sci.* **2009**, *337*, 396–407.

(39) Kozlova, N.; Santore, M. M. Micrometer scale adhesion on nanometer-scale patchy surfaces: adhesion rates, adhesion thresholds, and curvature-based selectivity. *Langmuir* **2007**, *23*, 4782–4791.

(40) Kalasin, S.; Santore, M. M. Hydrodynamic crossover in dynamic microparticle adhesion on surfaces of controlled nanoscale heterogeneity. *Langmuir* **2008**, *24*, 4435–4438.

(41) Hoek, E. M. V.; Agarwal, G. K. Extended DLVO interactions between spherical particles and rough surfaces. *J. Colloid Interface Sci.* **2006**, *298*, 50–58.